Desalination and Water Treatment
www.deswater.com
doi: 10.1080/19443994.2013.873350

53 (2015) 3632–3640
March

Taylor & Francis
Taylor & Francis Group

Plasma activation and acrylic acid grafting on polypropylene nonwoven surface for the removal of cationic dye from aqueous media

Aminoddin Haji[a], Ahmad Mousavi Shoushtari[a,*], Majid Abdouss[b]

[a]*Textile Engineering Department, Amirkabir University of Technology, Tehran, Iran*
Tel. +98 2164542638; Fax: +98 2166400245; email: amousavi@aut.ac.ir
[b]*Chemistry Department, Amirkabir University of Technology, Tehran, Iran*

Received 2 July 2013; Accepted 2 December 2013

ABSTRACT

In this paper, the preparation, characterization and cationic dye adsorption properties of acrylic acid-grafted polypropylene nonwoven (AA-PP) using plasma as a surface activation pretreatment were investigated. Surface characteristics of AA-PP were studied using attenuated total reflection–Fourier transform infrared spectroscopy and scanning electron microscopy. Methylene blue was used as a model dye. The effects of operational parameters such as AA-PP dosage, initial dye concentration, and pH on dye removal were evaluated. The isotherm and kinetics of dye adsorption were also studied. The data were evaluated for compliance with the Langmuir, Freundlich, and Temkin isotherm models. It was found that the dye adsorption followed Freundlich isotherm. The rates of sorption were found to conform to pseudo-first-order kinetics with good correlation. Results indicated that AA-PP could be used as a cheap, long–lasting, and more environmentally friendly sorbent to remove cationic organics from contaminated water, compared to other adsorbents.

Keywords: Plasma; Acrylic acid; Polypropylene; Grafting; Dye removal

1. Introduction

The presence of dyes and pigments in water, even at low concentrations, is highly visible, undesirable, and worrying for both toxicological and esthetical reasons [1,2]. Colored effluents are mainly repelled from textile companies, dye manufacturing industries, pulp mills, tanneries, electroplating factories, and food companies [2,3]. Due to complex aromatic structures, synthetic dyes are more stable to light, heat, chemical, and biological degradation [1–3]. Several methods including adsorption on various sorbents [3], nanofiltration [4], chemical decomposition by ozonation [5], electrocoagulation [6], photodegradation [7], microbiological decoloration [8], employing activated sludge [9], pure cultures, and microbe consortiums [10,11] have been presented for dye removal from wastewater.

Among these processes, adsorption has several advantages compared to other techniques in terms of high removal efficiency, ease of operation, simplicity of design, initial cost, and insensitivity of toxic substances [2,12]. This has made it the most economical and effective treatment method for the removal of dyes [13]. Several types of adsorbents have been applied for the adsorption of dyes from aqueous solutions, including polymers, biopolymers, activated

*Corresponding author.

carbon, wood, agricultural wastes, hydrogels, activated red mud, clay, etc. [3,13].

Polymeric fibers have been used as adsorbents for removing dyes and metal ions from water or wastewater in recent years [14,15]. They have relatively large specific surface areas, high adsorption kinetics, and low cost, which has made them favorable for wastewater treatment [13].

Polypropylene fiber (PP) has outstanding properties such as chemical and physical stability, good resistance to biodegradation, easy processability, and low manufacturing costs. However, the lack of functional sites and highly crystalline structure of PP molecular chains have decreased its performance in some applications [16].

This material cannot absorb either dye cations or anions. Certain desirable properties such as improved dyeability, water absorbency, antistatic, mechanical, and thermal properties can be imparted to PP fibers through grafting with different vinyl monomers. Grafting can significantly improve the dye selectivity and its adsorption capacity to fibers by forming reactive groups on the polymer chains [17].

Graft copolymerization can be initiated using photo irradiation, gamma rays, electron beam, ultraviolet light (UV), plasma treatment, or chemical initiators [17,18]. Among these methods, plasma treatment is one of the most convenient methods, due to the ease of creation of active sites needed to initiate the grafting. Also, it is an alternative environmentally friendlier method compared with the traditional chemical activation which only affects the uppermost atomic layers of a material surface without changing the bulk properties [19–21].

Plasma is a gaseous mixture consisting of electrons, equally charged ions, molecules, and atoms and many reactions occur simultaneously in a plasma system. Plasma treatment is employed as an effective way to modify the surface of textile materials to enhance properties like water absorbency, water repellency, yarn spinning properties, antibacterial properties, dirt release, dyeing, shrinking, form retention, etc. [19–25].

The plasma treatment effects on PP fibers decrease more or less rapidly and furthermore, do not generate a sufficient density of functional groups on the fiber surface. So, grafting of acrylic acid (AA) on the fibers surfaces can be considered as a strategy that leads to a coating rich in functional groups [23].

Several studies have been done on grafting of AA onto PP surface using plasma treatment [22]. They generally have focused on studying the effect of process parameters on the degree of grafting and properties of the grafted substrate [23]. In some studies, AA grafting has been used to immobilize bioactive compounds on the surface of PP [23–25]. AA-grafted polypropylene nonwovens (AA-PPs) have been used to remove cations [26] and organic pollutants from water [27].

In this study, AA was grafted on PP nonwoven using plasma activation. The process of AA grafting consists of two steps: (1) oxygen plasma activation of the PP surface; and (2) immersion of the pre-activated substrate in an AA solution to graft poly(AA) on it. This method has been optimized using an experimental design, varying the monomer concentration, time of immersion, plasma power, duration of plasma treatment, and grafting temperature, in order to obtain the optimum grafting yield regarding the maximum surface carboxylic groups content [28]. Samples were prepared in optimal conditions. A comprehensive attempt has been made on the studying of the adsorption of methylene blue (MB) as a model cationic dye on the modified PP nonwoven.

2. Materials and methods

2.1. Materials

PP nonwoven with thickness of 109 μm and density of 20 g/m^2 was obtained from a local mill. Before plasma treatment, to remove the spin finish, all samples ($5 \times 7\ cm^2$) were washed in ethanol for 30 min at ambient temperature, rinsed with distilled water, and finally dried at 50 °C. All chemicals used were of analytical grade and obtained from Merck.

2.2. Methods

2.2.1. Preparation of AA-PP

To produce peroxide radicals required for grafting of AA on the surface of PP nonwoven [25,29], plasma treatment was carried out using a low-pressure radio frequency (13.56 MHz) equipment (model: Junior advanced, Europlasma, Belgium). The system was evacuated to 100 mTorr and oxygen was introduced into the chamber at a flow rate of 20 sccm (standard cubic centimeters per minute). The chamber pressure was subsequently maintained at 100 mTorr and plasma was generated at 100 W for 1 min. Subsequently, air was introduced into the chamber and the sample was removed for the grafting reaction. The time between the plasma treatment and the beginning of the grafting reaction was around 5 min.

Prior to enter the plasma-treated samples in the grafting solution (30% V/V AA in water), the solution was deaerated with nitrogen bubbling through it

for 1 h. The grafting process was carried out at 65°C for 1 h. After grafting, the residual monomers and homopolymers were removed from the surface of the fibers by washing in boiling water for 30 min.

The grafting yield was calculated according to Eq. (1):

$$G.Y\,\% = [(W_1 - W_2)/W_1] \times 100 \quad (1)$$

where W_1 and W_2 are the weight of PP non-woven sample before and after grafting, respectively. In this study, the grafting yield was 35%.

2.2.2. ATR–FTIR analysis

The introduction of functional groups onto the surface of PP nonwoven was confirmed by attenuated reflectance–Fourier transform infrared spectroscopy (ATR–FTIR) analysis using a Nicolet 670 spectrometer with a resolution of 4 cm^{-1}. An average of 40 scans was recorded.

2.2.2.1. Scanning electron microscopy observation. The surface morphology of raw- and AA-grafted PP nonwovens was studied using an AIS2100 SEM (Seron Technology, South Korea) after coating the samples with gold.

2.2.3. Adsorption procedure

The dye adsorption measurements were conducted in jars containing 50 mL of MB solutions with different concentrations in contact with various amounts of AA-PP. The solution pH was adjusted by adding a few drops of dilute solutions of H_2SO_4 or NaOH. The changes in the absorbance of all solution samples were determined at certain time intervals during the adsorption process. The results were verified with the adsorption isotherms.

Jenway 6305 UV–vis spectrophotometer was employed for absorbance measurements. The maximum wavelength (λ_{max}) used for the determination of residual concentration of MB in supernatant solutions using UV–vis spectrophotometer was 662 nm. A calibration curve was first generated from the optical density of MB solutions of known concentrations at 662 nm measured on the same spectrophotometer. The procedure of colorimetric analysis was done three times for each sample and an average of three measurements was recorded.

The effect of AA-PP dosages on dye removal was investigated by contacting 50 mL of dye solution with initial dye concentration of 10 mg/L and pH = 11 using jar test at room temperature (25°C) for different times at a constant stirring speed of 200 rpm. Different amounts of AA-PP (0.01–0.1 g) were applied to remove MB from water.

The effect of pH on dye removal was investigated by contacting 50 mL of dye solution with AA-PP (0.02 g) and initial dye concentration (10 mg/L) using jar test at room temperature (25°C) for 2 and 24 h at a constant stirring speed of 200 rpm. Different pH values (3, 5, 7, 9, and 11) were applied to remove MB from water.

The effect of initial dye concentration on dye removal was investigated by contacting 50 mL of dye solution with AA-PP (0.02 g) and pH = 11 using jar test at room temperature (25°C) for 90 min at a constant stirring speed of 200 rpm. Different initial dye concentrations (2, 5, 10, and 15 mg/L) were applied.

3. Results and discussion

3.1. Characterization of AA-PP

In order to investigate the surface characteristics of AA-PP, ATR–FTIR spectra, and SEM images were studied. Fig. 1 shows the ATR–FTIR spectra of the virgin and AA-PP nonwoven. It shows the characteristic peaks of raw PP in the region 2,800–3,000 cm^{-1} (2,950, 2,915, 2,870, and 2,837 cm^{-1}). The peaks at 2,950 and 2,870 cm^{-1} are due to the asymmetric and symmetric stretching vibrations of methyl group, respectively. The peaks at 2,915 and 2,837 cm^{-1} may be ascribed to the $-CH_2$ asymmetric and symmetric stretching vibrations, respectively. The original PP shows two distinct peaks at 1,449 and 1,371 cm^{-1} which are due to the asymmetric and symmetric bending vibrations of methyl groups, respectively. The grafting of AA results in the appearance of new peaks. A new broad peak has arisen between 3,000 and 3,600 cm^{-1} due to –OH stretching vibrations from the carboxyl groups. The broad peak indicates the hydrogen bonding among the carboxyl groups. The formation of the peak at 1,700 cm^{-1} may be attributed to the carbonyl stretching vibration of the carboxyl group. This confirms the grafting of poly(AA) chains on the fibers' surfaces. There is another peak originating at 1,412 cm^{-1}. This peak is related to the in-plane O–H bending vibration. The presence of a peak at 1,550 cm^{-1} in the grafted sample can be attributed to the carboxylate ion [30].

Scanning electron micrographs of PP and AA-PP are shown in Fig. 2. It is clear that AA has been grafted on the surface of PP fibers. The surface of raw

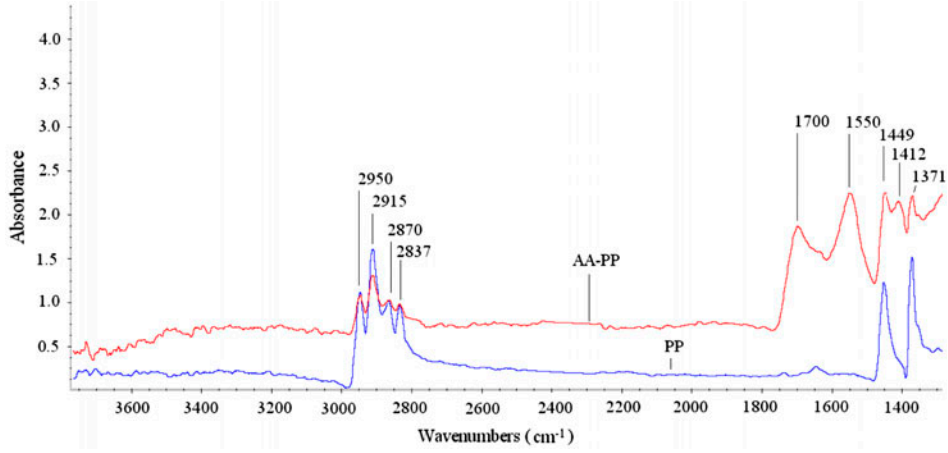

Fig. 1. ATR–FTIR spectra of the virgin (PP) and AA-grafted PP nonwoven (AA-PP).

PP fibers has a smooth and highly homogeneous appearance which has turned into rough after grafting of AA.

3.2. Effect of operational parameters on dye removal by AA-PP

3.2.1. Effect of adsorbent dosage

The plot of dye removal (%) vs. time (min) at different AA-PP dosages (g) is shown in Fig. 3. The initial dye concentration decreased rapidly with the contact time confirming strong interactions between the dye and the functional sites on the surface of AA-PP. In other words, the adsorption capacity increased with contact time. Maximum dye was adsorbed from the solution within 120 min. After that, the concentration of dye in the liquid phase remained almost constant. In fact, this observation indicates that adsorption is increased instantly at initial stages due to rapid attachment of dye to the surface of the AA-PP, and keeps increasing gradually until the equilibrium is reached, then remains constant after about 120 min. The amount of adsorbed dye showed no significant difference when the contact times were longer. So, 120 min was found to be sufficient for reaching the adsorption equilibrium for MB. These kinetic measurements showed that the process was rapid. The process was also uniform; the time profile of dye uptake was a single, smooth, and continuous curve leading to saturation, suggesting the possible monolayer coverage of dye on the surface of the AA-PP [31].

The increase in dye adsorption with adsorbent dosage can be attributed to increased adsorbent surface and availability of more adsorption sites (–COOH groups).

Regarding to our preliminary studies, no adsorption of dyes was observed on raw PP nonwoven at different values of pH. This confirms the role of –COOH sites of AA-PP in the adsorption of MB.

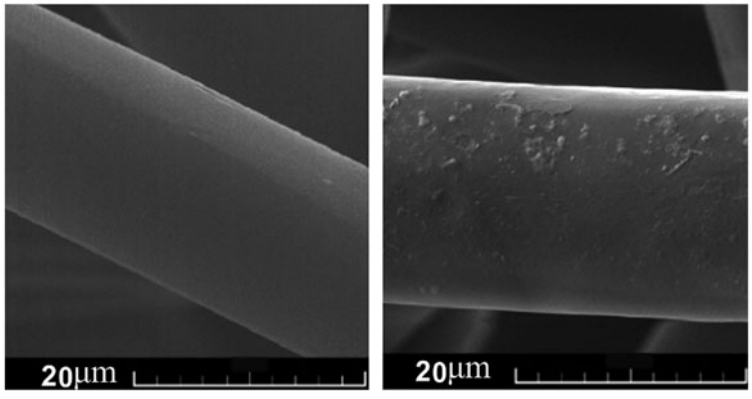

Fig. 2. Scanning electron micrographs of PP (left) and AA-PP (right).

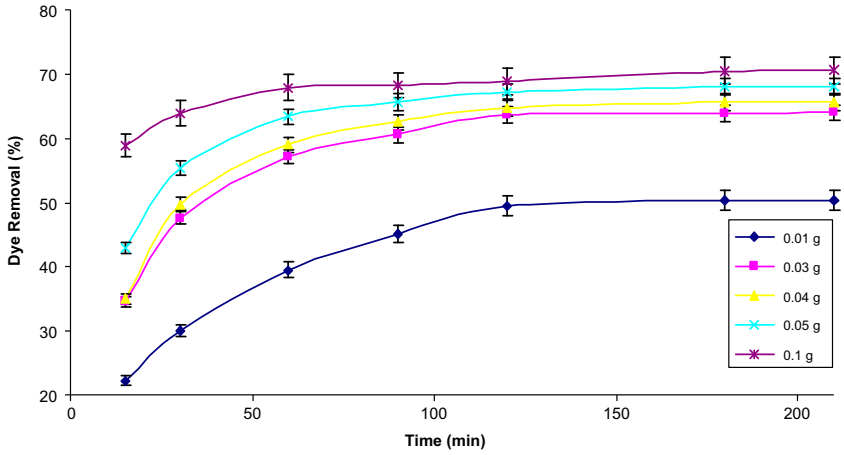

Fig. 3. The effect of AA-PP dosage (g) on dye removal (%) at different times (50 mL of 10 mg/L solution, pH = 11, 25°C).

3.2.2. Effect of pH

The effect of pH on the adsorption of MB onto AA-PP is shown in Fig. 4. The adsorption capacity increases when the pH is increased from 3 to 11. Maximum adsorption of MB occurs at alkali pH (pH 11). At various pH values, the electrostatic attraction as well as the organic property and structure of dye molecules and AA-PP could play very important roles in dye adsorption. At pH 11, a significant electrostatic attraction forms between the negatively charged surfaces of the adsorbent, due to the ionization of functional groups of adsorbent and positively charged cationic dye (Fig. 5). As the pH of the system decreases, the number of positively charged sites is decreased and consequently, lower adsorption of MB is observed.

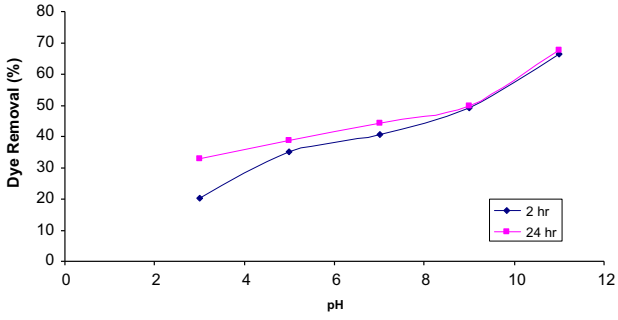

Fig. 4. The effect of pH on the adsorption of MB onto AA-PP (AA-PP = 0.02 g, 50 mL of 10 mg/L solution at 25°C for duration of 2 and 24 h).

3.2.3. Effect of dye concentration

The influence of varying the initial dye concentration on the adsorption of the dye was assessed. The results are shown in Fig. 6. It is obvious that the higher the initial dye concentration, the higher the percentage of adsorbed dye.

The adsorbed dye onto AA-PP increases with an increase in the initial dye concentration if the amount of adsorbent is kept unchanged due to the increase in the driving force of the concentration gradient with the higher initial dye concentration. This confirmed the strong chemical interactions between the basic dye and AA-PP [31].

3.3. Adsorption isotherm

The adsorption isotherm expresses the relation between the mass of the adsorbed dye at a particular temperature, pH, particle size, and liquid phase of the dye concentration.

The Langmuir isotherm which has been successfully applied to many adsorption processes can be used to explain the adsorption of dye into adsorbent. A basic assumption of the Langmuir theory is that adsorption takes place at specific sites within the adsorbent [3,32]. The Langmuir equation can be written as follows:

$$q_e = Q_0 K_L C_e / 1 + K_L C_e \quad (2)$$

where q_e, C_e, K_L, and Q_0 are the amount of dye adsorbed on AA-PP at equilibrium (mg/g), the Langmuir concentration of dye solution (mg/L),

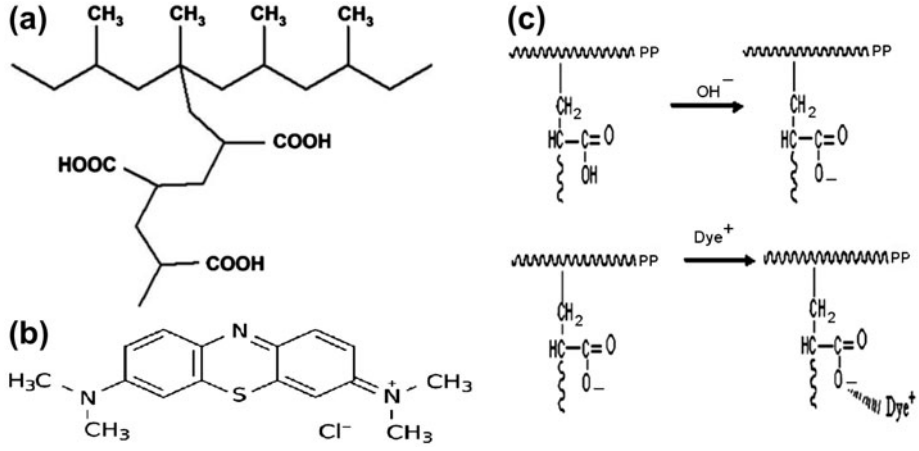

Fig. 5. Chemical structures of (a) AA-PP, (b) MB, and (c) schematic mechanism of adsorption of a cationic dye on AA-PP.

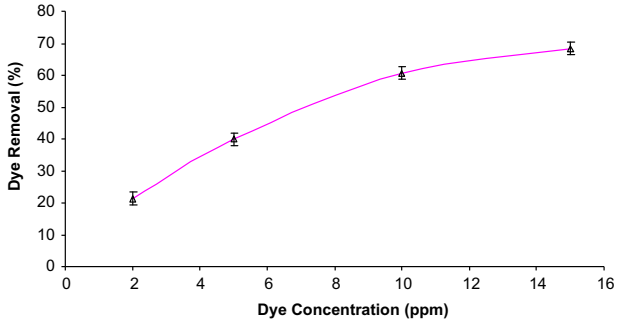

Fig. 6. The influence of initial dye concentration on the adsorption of MB (AA-PP = 0.02 g, 50 mL solution, pH = 11, 2 ℃, 90 min).

equilibrium constant (L/g), and the maximum adsorption capacity (mg/g), respectively [3,5,33].

The linear form of Langmuir equation is:

$$C_e/q_e = 1/K_L Q_0 + C_e/Q_0 \tag{3}$$

Also, Isotherm data were evaluated with Freundlich isotherm that can be expressed by [3,32]:

$$q_e = K_F C_e^{1/n} \tag{4}$$

where K_F is adsorption capacity at unit concentration and $1/n$ is adsorption intensity.

$1/n$ values indicate the type of isotherm to be irreversible ($1/n = 0$), favorable ($0 < 1/n < 1$), and unfavorable ($1/n > 1$). Eq. (3) can be rearranged to a linear form [34]:

$$\log q_e = \log K_F + (1/n) \log C_e \tag{5}$$

The Temkin isotherm is given as:

$$Q_e = RT/b \ln (K_T C_e) \tag{6}$$

which can be linearized as:

$$q_e = B_1 \ln K_T + B_1 \ln C_e \tag{7}$$

where

$$B_1 = RT/b \tag{8}$$

Temkin isotherm contains a factor that explicitly takes into account the interactions between the adsorbing species and the adsorbent. This isotherm assumes that (1) the heat of adsorption of all the molecules in the layer decreases linearly with coverage due to adsorbent–adsorbate interactions, and that (2) the adsorption is characterized by a uniform distribution of binding energies, up to some maximum binding energy. A plot of q_e vs. ln C_e enables the determination of the isotherm constants B_1 and K_T from the slope and the intercept, respectively. K_T is the equilibrium binding constant (L/mol) corresponding to the maximum binding energy and constant B_1 is related to the heat of adsorption [35].

To study the applicability of the Langmuir, Freundlich, and Temkin isotherms for the dye adsorption onto AA-PP at different dye concentrations, linear plots of C_e/q_e against C_e, log q_e vs. log C_e, and q_e vs. ln C_e are ploted and shown in Figs. 7–9, respectively. The values of Q_0, K_L, K_F, $1/n$, K_T, B_1, and

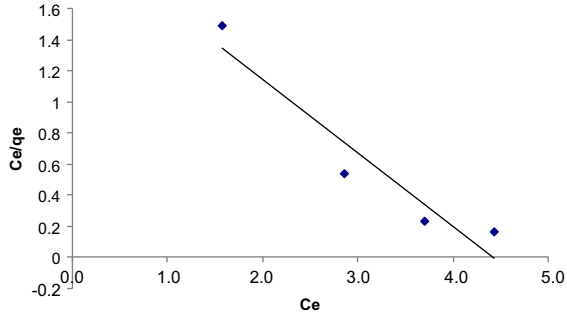

Fig. 7. Langmuir adsorption isotherm of MB adsorption onto AA-PP.

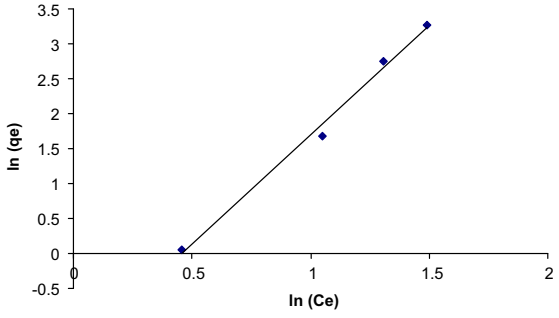

Fig. 8. Freundlich adsorption isotherm of MB adsorption onto AA-PP.

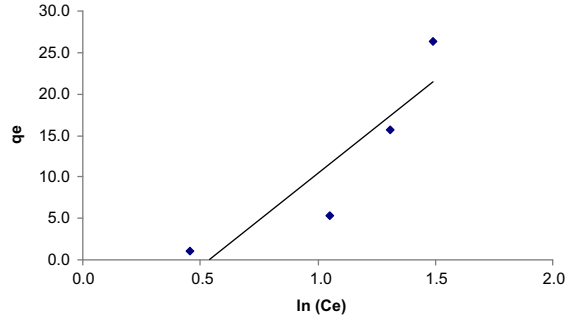

Fig. 9. Temkin adsorption isotherm of MB adsorption onto AA-PP.

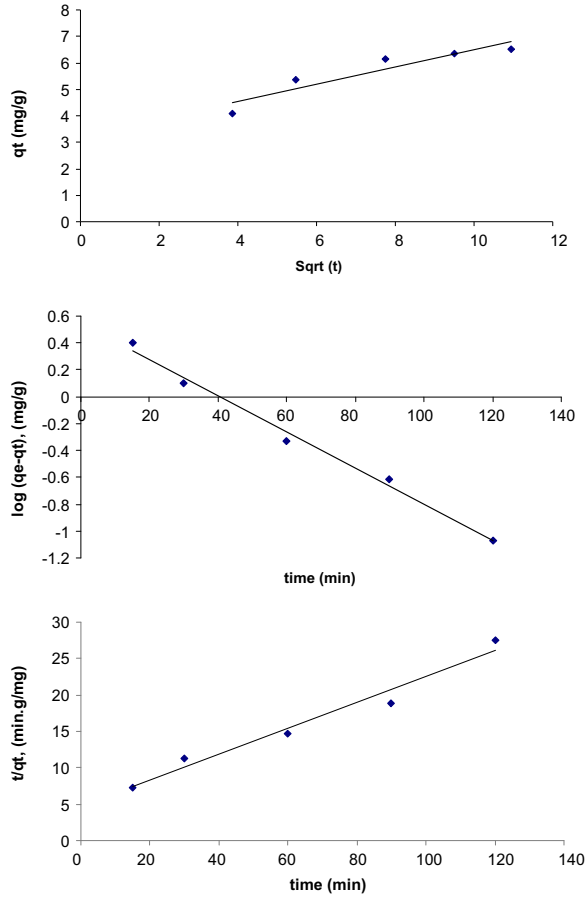

Fig. 10. Intraparticle diffusion (top), pseudo-first-order (middle), and pseudo-second-order (down) models for the MB dye adsorption onto AA-PP.

R^2 (correlation coefficient values of all isotherms models) are shown in Table 1.

The correlation coefficient values (R^2) show that the dye removal isotherm using AA-PP does not follow the Langmuir and Temkin isotherms (Table 1). The linear fit and calculated correlation coefficients (R^2) for Freundlich isotherm model show that the dye removal isotherm can be approximated as Freundlich model (Table 1). This means that the adsorption of dyes takes place at specific heterogeneous sites and a one-layer adsorption onto AA-PP surface [3].

Table 1
Linearized isotherm coefficients for dye adsorption onto AA-PP at different dye concentrations

Langmuir			Freundlich			Temkin		
Q_0	K_L	R^2	K_F	$1/n$	R^2	K_T	B_1	R^2
−2.114	−0.2258	0.9083	0.238	3.136	0.9918	0.5839	22.55	0.8058

Table 2
Linearized kinetic coefficients for dye adsorption onto AA-PP

Intraparticle diffusion			Pseudo-first-order		Pseudo-second-order	
k_p	I	R^2	k_1	R^2	k_2	R^2
0.3272	3.2366	0.8768	0.0308	0.9908	0.0067	0.9678

3.4. Adsorption kinetic

Several models can be used to express the mechanism of solute sorption onto a sorbent. In order to investigate the mechanism of adsorption, characteristic constants of adsorption were determined using intraparticle diffusion, pseudo-first-order and pseudo-second-order equations [3].

The possibility of intraparticle diffusion resistance affecting adsorption was explored by using the intraparticle diffusion model as:

$$q_t = k_p t^{1/2} + I \tag{9}$$

where k_p and I are the intraparticle diffusion rate constant and intercept, respectively.

Values of I give an idea about the thickness of the boundary layer, i.e. the larger the intercept, the greater is the boundary layer effect. According to this model, the plot of uptake should be linear if intraparticle diffusion is involved in the adsorption process and if these lines pass through the origin then intraparticle diffusion is the rate controlling step. When the plots do not pass through the origin, this is indicative of some degree of boundary layer control and it shows that the intraparticle diffusion is not the only rate limiting step, but also other kinetic models may control the rate of adsorption, all of which may be operating simultaneously.

A linear form of pseudo-first-order model is:

$$\log(q_e - q_t) = \log(q_e) - (k_1/2.303)t \tag{10}$$

where q_e, q_t, and k_1 are the amount of dye adsorbed at equilibrium (mg/g), the amount of dye adsorbed at time t (mg/g), and is the equilibrium rate constant of pseudo-first-order kinetics (1/min), respectively. The linear fit between the log ($q_e - q_t$) and contact time (t) under pH 11 can be approximated as pseudo-first-order kinetics.

Linear form of pseudo-second-order model is illustrated as:

$$t/q_t = 1/k_2 q_e + (1/q_e)t \tag{11}$$

where k_2 is the equilibrium rate constant of pseudo-second-order (g/mg min) [3].

To understand the applicability of the intraparticle diffusion, pseudo-first-order and pseudo-second-order models for the dye adsorption onto AA-PP linear plots of q_t against $t^{1/2}$, log (q_e–q_t) vs. contact time (t) and t/q_t vs. contact time (t) are plotted (Fig. 10). The values of k_p, I, k_1, k_2, R^2 (correlation coefficient values of all kinetics models) are shown in Table 2.

The linear fit between the log ($q_e - q_t$) vs. contact time (t) and calculated correlation coefficient (R^2) for pseudo-first-order kinetics model show that the dye removal kinetic can be approximated as pseudo-first-order kinetics (Table 2 and Fig. 10).

4. Conclusion

The preparation, characterization, and dye adsorption properties of AA-PP were investigated. AA-PP was studied using FTIR and SEM. The formation of the peak at 1,700 cm^{-1} confirmed the grafting of poly (AA) chains on the fibers surfaces. The surface of AA grafted fibers was rough compared to the smooth and highly homogeneous appearance of raw PP fibers. Equilibrium studies were done for the adsorption of MB from aqueous solution onto AA-PP. The equilibrium data showed that adsorption of MB on AA-PP followed Freundlich isotherm. The data indicated that the adsorption kinetics of MB on AA-PP followed the pseudo-first-order model. The results showed that the AA-PP as a long-lasting and cost-effective adsorbent with relatively large adsorption capacity and might be a suitable alternative to remove cationic dyes from colored wastewater.

References

[1] L. Wang, J. Zhang, R. Zhao, C. Li, Y. Li, C. Zhang, Adsorption of basic dyes on activated carbon prepared from *Polygonum orientale* Linn: Equilibrium, kinetic and thermodynamic studies, Desalination 254 (2010) 68–74.
[2] N.K. Amin, Removal of reactive dye from aqueous solutions by adsorption onto activated carbons prepared from sugarcane bagasse pith, Desalination 223 (2008) 152–161.
[3] A. Haji, N.M. Mahmoodi, Soy meal hull activated carbon: Preparation, characterization and dye adsorption properties, Desalin. Water Treat. 44 (2012) 237–244.

[4] M. Khayet, M.N.A. Seman, N. Hilal, Response surface modeling and optimization of composite nanofiltration modified membranes, J. Membr. Sci. 349 (2010) 113–122.
[5] N.M. Mahmoodi, Photocatalytic ozonation of dyes using copper ferrite nanoparticle prepared by co-precipitation method, Desalination 279 (2011) 332–337.
[6] A.R. Amani-Ghadim, A. Olad, S. Aber, H. Ashassi-Sorkhabi, Comparison of organic dyes removal mechanism in electrocoagulation process using iron and aluminum anodes, Environ. Prog. Sustainable Energy 32 (2013) 547–556.
[7] B. Subash, B. Krishnakumar, R. Velmurugan, M. Swaminathan, Photodegradation of an azo dye with reusable SrF_2–TiO_2 under UV light and influence of operational parameters, Sep. Purif. Technol. 101 (2012) 98–106.
[8] R. Khan, P. Bhawana, M.H. Fulekar, Microbial decolorization and degradation of synthetic dyes: A review, Rev. Environ. Sci. Biotechnol. 12 (2013) 75–97.
[9] Y. Kang, T. Won, K. Hyun, Efficient treatment of real textile wastewater: Performance of activated sludge and biofilter systems with a high-rate filter as a pre-treatment process, KSCE J. Civ. Eng. 16 (2012) 308–315.
[10] Y. Patel, C. Mehta, A. Gupte, Assessment of biological decolorization and degradation of sulfonated di-azo dye acid maroon V by isolated bacterial consortium EDPA, Int. Biodeterior. Biodegrad. 75 (2012) 187–193.
[11] M.B. Kurade, T.R. Waghmode, A.N. Kagalkar, S.P. Govindwar, Decolorization of textile industry effluent containing disperse dye Scarlet RR by a newly developed bacterial-yeast consortium BL-GG, Chem. Eng. J. 184 (2012) 33–41.
[12] Y.H. Chen, Synthesis, characterization and dye adsorption of ilmenite nanoparticles, J. Non-Cryst. Solids 357 (2011) 136–139.
[13] M. Arslan, M. Yiğitoğlu, Use of methacrylic acid grafted poly(ethylene terephthalate) fibers for the removal of basic dyes from aqueous solutions, J. Appl. Polym. Sci. 110 (2008) 30–38.
[14] M. Abdouss, A. Mousavi Shoushtari, A. Haji, B. Moshref, Fabrication of chelating diethylenetriaminated pan micro and nano fibers for heavy metal removal, Chem. Indust. Chem. Eng. Q. 18 (2012) 27–34.
[15] C. Guo, Q. Kong, J. Gao, Q. Ji, Y. Xia, Removal of methylene blue dye from simulated wastewater by alginic acid fiber as adsorbent: Equilibrium, kinetic, and thermodynamic studies, Can. J. Chem. Eng. 89 (2011) 1545–1553.
[16] A. Bhattacharya, B.N. Misra, Grafting: A versatile means to modify polymers techniques, factors and applications, Prog. Polym. Sci. 29 (2004) 767–814.
[17] S.D. Bhattacharya, M.S. Inamdar, Polyacrylic acid grafting onto isotactic polypropylene fiber: Methods, characterization, and properties, J. Appl. Polym. Sci. 103 (2007) 1152–1165.
[18] H.-J. Park, C.-K. Na, Preparation of anion exchanger by amination of acrylic acid grafted polypropylene nonwoven fiber and its ion-exchange property, J. Colloid Interface Sci. 301 (2006) 46–54.
[19] W.S. Man, C.W. Kan, S.P. Ng, The use of atmospheric pressure plasma treatment on enhancing the pigment application to cotton fabric, Vacuum. 99 (2014) 7–11.
[20] K. Wang, W. Wang, D. Yang, Y. Huo, D. Wang, Surface modification of polypropylene non-woven fabric using atmospheric nitrogen dielectric barrier discharge plasma, Appl. Surf. Sci. 256 (2010) 6859–6864.
[21] J. López-García, F. Bílek, M. Lehocký, I. Junkar, M. Mozetič, M. Sowe, Enhanced printability of polyethylene through air plasma treatment, Vacuum 95 (2013) 43–49.
[22] S. Saxena, A.R. Ray, A. Kapil, G. Pavon-Djavid, D. Letourneur, B. Gupta, A. Meddahi-Pellé, Development of a new polypropylene-based suture: Plasma grafting, surface treatment, characterization, and biocompatibility studies, Macromol. Biosci. 11 (2011) 373–382.
[23] S. Degoutin, M. Jimenez, M. Casetta, S. Bellayer, F. Chai, N. Blanchemain, C. Neut, I. Kacem, M. Traisnel, B. Martel, Anticoagulant and antimicrobial finishing of non-woven polypropylene textiles, Biomed. Mater. 7 (2012) 035001–035013.
[24] D.M. Wafa, F. Breidt, S.M. Gawish, S.R. Matthews, K.V. Donohue, R.M. Roe, M.A. Bourham, Atmospheric plasma-aided biocidal finishes for nonwoven polypropylene fabrics. II. Functionality of synthesized fabrics, J. Appl. Polym. Sci. 103 (2007) 1911–1917.
[25] K.S. Siow, L. Britcher, S. Kumar, H.J. Griesser, Plasma methods for the generation of chemically reactive surfaces for biomolecule immobilization and cell colonization—A review, Plasma Processes Polym. 3 (2006) 392–418.
[26] L. Wei, J. Wei, F. Yuan, J. Dong, Preparation and characterization of nonwoven polypropylene fabric irradiation-grafted with acrylic acid as weakly acidic cation exchange fiber, Int. J. Chem. 1 (2009) 60–67.
[27] H.M. Said, H.H. Sokker, A. El-Hag Ali, Acrylation of pre-irradiated polypropylene and its application for removal of organic pollutants, Radiat. Phys. Chem. 79 (2010) 534–539.
[28] A. Haji, Application of amine nanodendrimer on PP nonwoven using oxygen plasma and evaluating the adsorption properties, PhD thesis, Textile Engineering Department, Amirkabir University of Technology, Tehran, 2012.
[29] J. Wang, X. Liu, H.-S. Choi, Graft copolymerization kinetics of acrylic acid onto the poly(ethylene terephthalate) surface by atmospheric pressure plasma inducement, J. Polym. Sci., Part B: Polym. Phys. 46 (2008) 1594–1601.
[30] S. Saxena, A.R. Ray, B. Gupta, Chitosan immobilization on polyAA grafted polypropylene monofilament, Carbohydr. Polym. 82 (2010) 1315–1322.
[31] G. Crini, Kinetic and equilibrium studies on the removal of cationic dyes from aqueous solution by adsorption onto a cyclodextrin polymer, Dyes Pigm. 77 (2008) 415–426.
[32] M. Zargaran, A.M. Shoushtari, M. Abdouss, Studies on sorption isotherm models of ion exchange modified acrylic fibers, J. Appl. Polym. Sci. 118 (2010) 135–142.
[33] I. Langmuir, The constitution and fundamental properties of solids and liquids. Part I. Solids, J. Am. Chem. Soc. 38 (1916) 2221–2295.
[34] H.M.F. Freundlich, Über die adsorption in lösungen [About the adsorption in solutions], J. Phys. Chem. 57 (1906) 385–470.
[35] M.J. Temkin, V. Pyzhev, Recent modifications to Langmuir isotherms, Acta Physiochimica URSS 1 (1940) 217–222.